ADVANCED MATERIALS TECHNOLOGIES
www.advmattechnol.d

Biomimetic Graphene Actuators Enabled by Multiresponse Graphene Oxide Paper with Pretailored Reduction Gradient

Dong-Dong Han, Yu-Qing Liu, Jia-Nan Ma, Jiang-Wei Mao, Zhao-Di Chen, Yong-Lai Zhang, and Hong-Bo Sun*

The strong interaction between water molecules and graphene oxide (GO) enables moisture-responsive graphene actuators, revealing great potential for soft robots. However, current strategies for developing smart graphene actuators fail to tailor their material property gradient in a controlled manner, and the driving manner is usually limited to single stimulus actuation. Here, a facile preparation of humidity/thermal/light multiresponsive graphene actuators by sequential vacuum filtration of GO and reduced GO (RGO) aqueous solutions is reported. The photoreduction degree of RGO layer is tuned precisely beforehand by changing ultraviolet (UV) light irradiation time, and thus a pretailored reduction gradient along the normal direction of the GO/RGO bilayer paper would form in a highly controlled manner. Taking advantage of the competitive water adsorption between the GO and RGO layers, as well as the thermal-, light-promoted desorption, the GO/RGO bilayers deform in response to moisture, light, and temperature changes; and the deformation degree can be modulated by controlling the gradient of oxygen-containing groups (OCGs). As a proof of principle, a humidity-responsive graphene mimosa and a humidity/thermal/light multiresponsive graphene actuators are fabricated. The GO/RGO bilayer paper with pretailored reduction gradient holds great promise for easy fabrication of biomimetic actuators that enable performing predictable deformation.

Stimuli-responsive materials (SRMs)[1] that can deform themselves and perform special motions under external stimuli have revealed great potential for versatile applications ranging from energy conversion devices, artificial muscles, to robotics.[2] As a main type of SRMs, bi/multilayer materials have been intensively investigated due to their fast and reversible response to surroundings, as well as large-scale and controllable deformation.[3] A basic working principle for such bi-/multilayer SRMs is the asymmetric expansions/contractions among different material layers.[4] According to this guideline, bi-/multilayer SRMs that enables bending, twisting, folding, and even origami at micro/nanoscale have been successfully developed based on a wide range of functional materials. For examples, Gracias and co-workers successfully developed a series of stimuli-responsive μ-grippers with bilayer structures for biomedical applications.[5] Zhang et al. reported SiGe/Si/Cr helical coils and Si/Cr μ-claw by the edge effect.[6] Hayward and co-workers fabricated thermally actuated μ-Randlett's flapping bird with poly(*p*-methylstyrene)/poly(*N*-isopropyl acrylamide-*co*-sodium acrylate)/poly(*p*-methylstyrene) trilayer structures.[7] To date, despite the fact that various bi-/multilayer SRMs have been well designed and prepared by rational assembly of different material layers, continued efforts in developing novel materials systems for multiresponsive actuation are still highly desired.

Recently, graphene and its derivatives (e.g., graphene oxide, GO) have been considered ideal candidates to make bi-/multilayer SRMs, since they are natural 2D materials that possess fascinating characteristics such as flexibility, conductivity, transparency, excellent stability, biocompatibility, and several unique chemical/physical properties.[8] Notably, GO is very sensitive to environmental humidity due to the presence of a large amount of oxygen-containing groups (OCGs).[9] Previously, Okuzaki et al. had reported that conducting polymers possessing plenty of hydrophilic functional groups, such as polypyrrole and poly(3,4-ethylenedioxythiophene)/poly(4-styrene sulfonate) films,[10–12] are moisture responsive and can be employed for developing soft actuators. Similar with these conducting polymers that can deform upon sorption and desorption of water, GO is also moisture responsive. The adsorption, desorption, and free permeation of water molecules make GO very promising for humidity sensors,[13] generators,[14] motors,[15] and functional membranes used for sea water desalinization.[16] Owing to the strong interaction with water molecules, GO has also been successfully employed to fabricate humidity-responsive actuators. As a pioneer work, Qu and co-workers first fabricated fiber-type moisture-responsive graphene actuators by selective laser reduction of GO fibers, in which

Dr. D.-D. Han, Y.-Q. Liu, J.-N. Ma, J.-W. Mao, Z.-D. Chen,
Prof. Y.-L. Zhang, Prof. H.-B. Sun
State Key Laboratory on Integrated Optoelectronics
College of Electronic Science and Engineering
Jilin University
Qianjin Street 2699, Changchun 130012, P. R. China
E-mail: yonglaizhang@jlu.edu.cn
Prof. H.-B. Sun
State Key Laboratory of Precision Measurement and Instruments
Department of Precision Instrument
Tsinghua University
Beijing 100084, P. R. China

DOI: 10.1002/admt.201800258

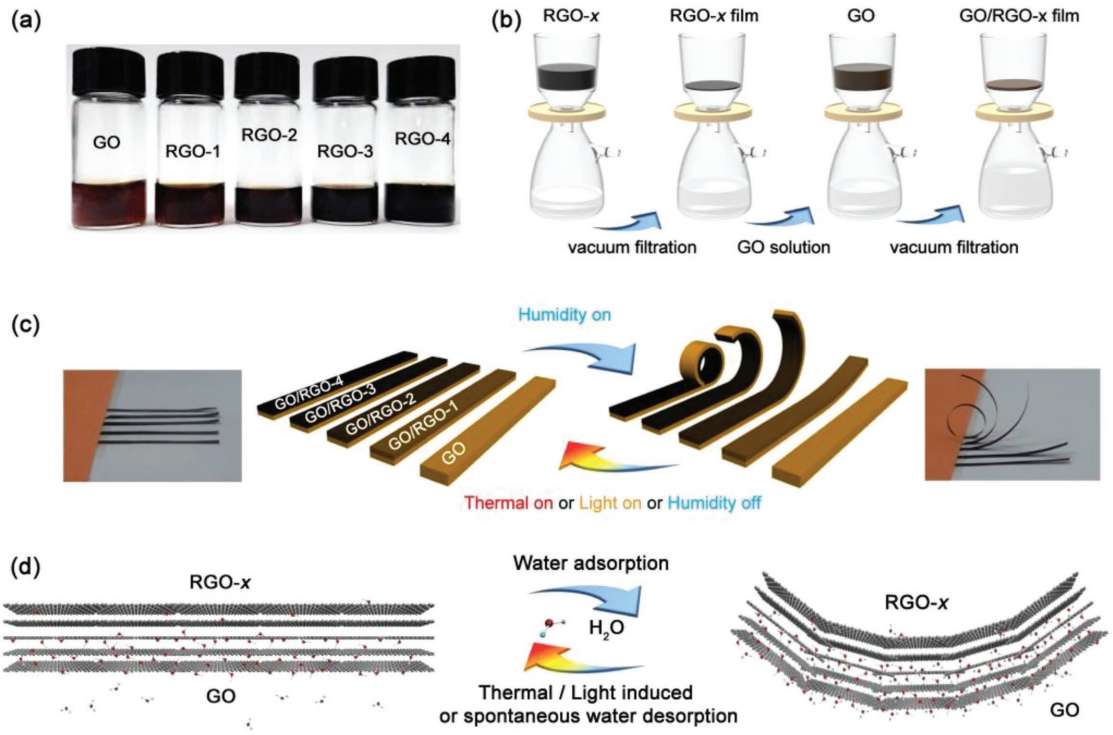

Figure 1. Schematic illustration of the fabrication of multiresponsive graphene actuators with predictable deformation. a) Photographs of GO and RGO-*x* solutions prepared by 1, 2, 3, and 4 h UV irradiation, respectively. b) The GO/RGO bilayer films were prepared by sequential vacuum filtration of RGO-*x* (*x* = 1–4 h) and GO, respectively. c) Schematic illustration and corresponding photographs of the reversible deformation of the multiresponsive GO/RGO-*x* ribbons. d) Schematic illustration of the responsive mechanism: competitive adsorption/desorption of water molecules between GO/RGO-*x* bilayers induced asymmetric volume changes.

predictable deformation including a folded, hook, S-shaped, and self-supporting spring structures can be achieved.[17] In our precious works, a self-controlled photoreduction treatment of GO using sunlight or UV irradiation as a light source has been proven workable to generate GO/RGO bilayers, enabling the development of paper-type moisture-responsive actuators.[18] Despite the fact that GO-based actuators can be fabricated by selective reduction of GO, current strategies mainly rely on the post-treatment of GO, which inevitably used special instruments and involved complex procedures. In most cases, it is really difficult to get precise control over the reduction gradient of GO, and thus the deformation degree of the resultant GO/RGO bilayer actuator is usually uncontrollable, which limits their practical application in robotics.

Actually, unlike the postreduction of solid GO films, the liquid-phase GO photoreduction protocol permits exquisite control over the contents of OCGs' residual on GO sheets by tuning the irradiation time continuously. In this regard, pretailoring the GO reduction gradient before the formation of bilayer structures seems a better way to control the deformation behavior of GO/RGO bilayer actuators. Herein, we report a very simple preparation of humidity/thermal/light multiresponsive graphene actuators by sequential vacuum filtration of GO and reduced GO (RGO) with pretailored reduction gradient. The development process of these actuators is both simple and ingenious, making it possible to prepare easily graphene-based actuators for which the deformation can be controlled. GO/RGO bilayer actuators with controllable deformation have been successfully fabricated for designing biomimetic paper robots. Taking advantage of the competitive water adsorption between the GO/RGO layers, and the thermal-, light-promoted water desorption processes, a multiresponsive insect-like graphene paper robot has been demonstrated as a proof of concept.

To get precise control over the reduction gradient, we first modulate the photoreduction degree of GO in aqueous solution by tuning the UV irradiation time from 1 to 4 h. As shown in **Figure 1**a, with the increase of irradiation time, the color of GO aqueous solution changes from yellowish brown to black gradually, indicating the reduction of GO. We selected four typical RGO samples named RGO-*x* (*x* is the photoreduction time in hour) for the fabrication of bilayer actuators. Figure 1b shows the preparation process, and four typical GO/RGO-*x* bilayer films were prepared by sequential vacuum filtration of RGO-*x* samples and pristine GO, respectively. After drying under ambient conditions, the GO/RGO-*x* bilayer films were peeled off for further usage.

Notably, the OCGs have strong interaction with water molecules, making GO and RGO very sensitive to the environmental humidity. Figure 1c shows the photographs and the schematic illustrations of a series of free-standing GO/RGO-*x* (*x* = 1, 2, 3, 4 h) ribbons at 33% RH (Figure 1c, left) and at 97% relative humidity (RH) (Figure 1c, right), respectively. For different bilayers, the curving degree is variable. By pretailoring the reduction degree of the RGO-*x* layer, a continuously tuned curving variation has been achieved. As compared with the postreduction method reported previously, the pretailored RGO

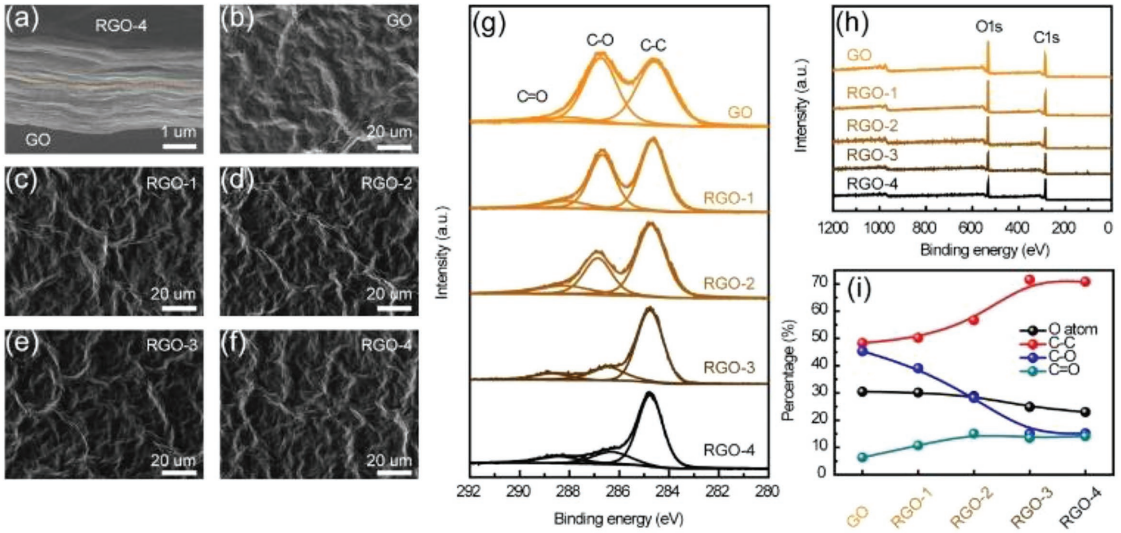

Figure 2. a) SEM image of the section view of GO/RGO-4 bilayer film. b–f) SEM images of GO, RGO-1, RGO-2, RGO-3, and RGO-4 surfaces, respectively. g) C1s XPS spectra of the GO side and RGO-*x* sides. h) Survey spectra of the GO side and RGO-*x* sides. i) Dependence of C—C, C—O, C=O, and O atom percentage of the GO side and RGO-*x* sides on UV irradiation time.

reduction degree enables more precise control over the OCG residuals and the deforming behavior. We explain the mechanism in Figure 1d. Generally, the layer where there exist more OCGs would show relative higher water adsorption capacity. For GO layer, the adsorption capability is constant; whereas in the RGO-*x* layer, the adsorption capacity is variable. Relative long time photoreduction treatment would result in less OCGs residuals, and therefore poorer water adsorption. The competitive water adsorption between the GO and RGO-*x* bilayers directly causes a mismatch in swelling degree, giving rise to a curving deformation toward the RGO side. In this regard, the precise control of the reduction degree of the RGO-*x* layer may govern the water adsorption capacity and influence the deforming behavior. Moreover, since water adsorption/desorption is reversible, the curving and straightening are also reversible. To promote the responsive properties, thermal or light stimuli could also be used to accelerate water desorption. In this way, humidity/thermal/light multiresponsive graphene actuators with tunable curving variation have been prepared by pretailoring the reduction gradient of GO.

The section and surface morphology of the GO/RGO-*x* (*x* = 1–4 h) bilayer film was analyzed using scanning electron microscopy (SEM) images. **Figure 2**a shows the cross-sectional SEM image of the GO/RGO-4 bilayer film. The thicknesses of both GO and RGO-*x* (*x* = 1–4 h) layers are controlled to be ≈1.3 µm. No obvious interface could be identified from the image since both GO and RGO-4 reveal a stacked layered structure. In addition, the surface morphology of GO and RGO is also quite similar. Figure 2b–f shows the top-view SEM images of the GO and RGO-*x* (*x* = 1–4 h) surfaces. Typical wrinkles can be observed from both GO and RGO sides.

X-ray photoelectron spectroscopy (XPS) was used to further evaluate the surface chemical compositions and functional groups of GO and RGO-*x* (*x* = 1–4 h). As shown in Figure 2g, the deconvoluted peaks of the C 1s spectra, centered at 284.6, 286.6, and 288.2 eV, represent the C—C (nonoxygen ring), C—O (hydroxyl and epoxy carbon), and C=O (carbonyl), respectively. The intensities of the peaks attributing to C—O decrease distinctly with the increasing of UV irradiation time, while the peak intensity corresponding to C=O decreases slightly. On the contrary, the content of carbon not bonded to oxygen grows prominently from 48.3% to 70.8%, indicating the gradually increased reduction degree of GO. As expected, for GO and RGO-*x* (*x* = 1–4 h), C 1s and O 1s signals were detected in the XPS survey spectra, respectively (Figure 2h). Peak analysis of the survey spectra revealed that the C/O atom ratio increased from 2.3 to 3.4, and the total O content reduced from 30.45% to 22.98 at% during 4 h UV irradiation, confirming the precise control over the OCGs' residual (Figure 2i). In our work, we found that further extending the irradiation time shows less obvious influence on the reduction degree. The RGO sample tends to be stable after 4 h irradiation. Therefore, in this work, the GO reduction degree can be continuously tuned within this range. However, it should be pointed out that the reduction degree could be further extended by using different light sources. Nevertheless, the thorough reduction of GO may result in poor solubility even flocculation from the solution, affecting the formation of smooth films. Besides, it is worth noting that GO prepared from different batches, or purchased from different suppliers, may have different O contents due to the different degrees of oxidation or using different graphite as raw materials. Thus, continuous control of the OCGs' residual and forming an obvious OCGs' gradient are quite important to realize the moisture-responsive properties.

The responsive properties of the GO/RGO-*x* (*x* = 1–4 h) bilayer actuators were carefully evaluated by changing the surrounding humidity, thermal, and light conditions. Under the humidity condition, GO/RGO-*x* bilayer films bend toward the RGO side because of the water adsorption–induced expansion of GO layer. As shown in **Figure 3**a, the curvature of GO/RGO-*x* bilayer ribbons (width 1.0 mm and length 12 mm) increased with the rise of environmental humidity from 33% RH to 97% RH. On the contrary, the GO single layer film (GO/RGO-0)

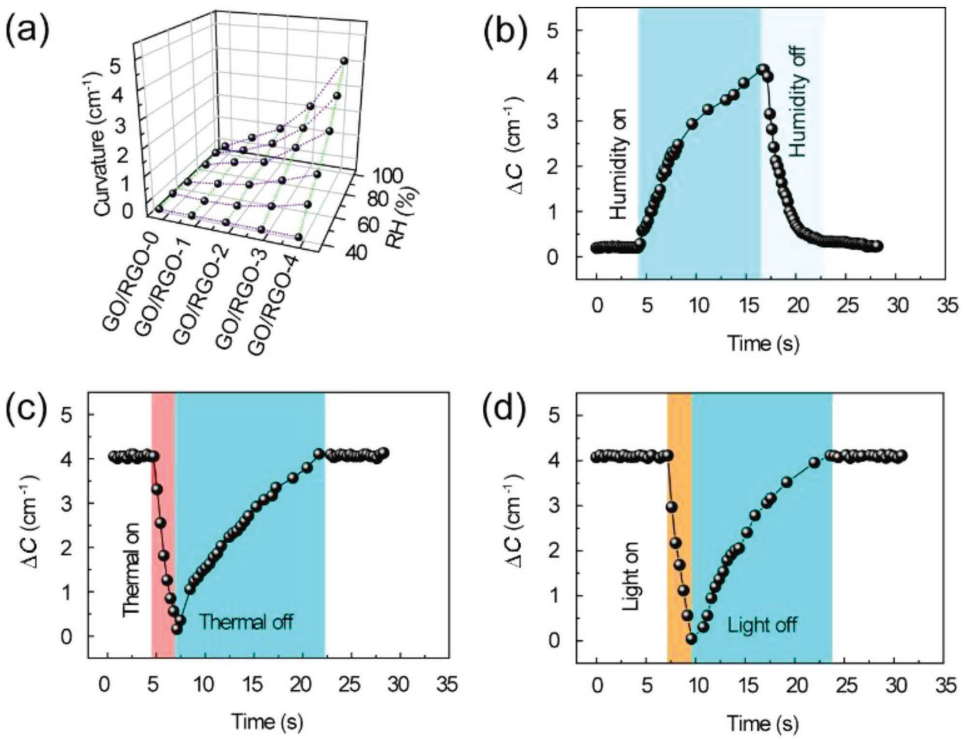

Figure 3. Humidity-, thermal-, and light-responsive properties of GO/RGO-4 films. a) Dependence of the curvature of the GO/RGO-*x* bilayer film on UV irradiation time and RH varies. b) Humidity-response and recovery properties of the GO/RGO-4 bilayer film. RH was switched between 33% and 97%. Δ*C* is the curvature variation. c) Thermal-response and recovery properties of the GO/RGO-4 bilayer film. Temperature was switched between 25 and 80 °C (RH = 97%). d) Light-response and recovery properties of the GO/RGO-4 bilayer film. The light intensity is ≈130 mW cm^{-2} (RH = 97%).

shows undetectable deformation under different humidity values. For different GO/RGO-*x* ribbons, the RGO layer prepared under long time photoreduction treatment shows a relative higher curving degree. A maximum curvature of ≈4.1 cm^{-1} was obtained in the case of GO/RGO-4 ribbon. Importantly, by tuning the photoreduction degree of the RGO layer, we can precisely control the curving degree of the bilayer ribbon at a certain RH. This is critical for further application is robot design, because, to realize complex performance, there is a need of employing a series of responsive ribbons with different deforming variations under a certain condition.

In this work, the GO/RGO bilayers are very sensitive the environmental humidity, and the response time is very short. Typical curvature–responsive time curve of GO/RGO-4 ribbon is shown in Figure 3b. The curvature of GO/RGO-4 increases from original value (≈0 cm^{-1}) to ≈4.1 cm^{-1} within ≈12 s when it was exposed to moisture (97% RH). The curvature restores its original value after the bilayer ribbon returns to ambient condition (33% RH) within ≈6 s. The response is so fast that for a bending and straightening cycle between 33% and 97% RH, it only takes less than 20 s. Moreover, the responsive properties are also very stable. The average curvature variation almost keeps a constant value between 33% and 95 % for 100 cycles, and the root mean square error (RMSE) of curvature for moisture, thermal, and light actuation for 100 cycles is calculated to be 0.086, 0.086, and 0.075, respectively (Figures S1–S3, Supporting Information). The response time can be further shortened by using thermal or light stimuli to accelerate the water desorption. When the temperature of the surrounding environment was increased to 80 °C, the curled of GO/RGO-4 ribbon (curvature variation, $\Delta C \approx 4$ cm^{-1}) turns to straight state rapidly with in 2.2 s (Figure 3c). When the hot plate was removed, the curvature recovered to the maximum value ($\Delta C \approx 4$ cm^{-1}) after ≈13 s. In addition to thermal effect, the photothermal effect of GO is also workable. Under light illumination, the photoenergy absorbed by GO can be converted to heat, which rises the local temperature and thus accelerates desorption of water molecules. The photothermal effect–induced water desorption can lead to obvious deformation of the GO/RGO bilayers. Under the illumination (light intensity ≈130 mW cm^{-2}), a curled GO/RGO-4 ribbon become straight in 2.6 s ($\Delta C \approx 4$ cm^{-1}), and after the removal of the light source, it recovered to curling state after ≈14 s (Figure 3d). In addition, we also test the curvature change between ambient condition (33% RH) and 40% RH for comparison (Figure S4, Supporting Information). Since the change of humidity is small, the deformation is not very obvious. The response time is even faster than that between 33% RH and 95% RH due to the relative small deformation degree.

To demonstrate the application of our humidity-responsive GO/RGO film in biomimetic actuators, we designed and fabricated two devices. As shown in **Figure 4**a, the first actuator was inspired from mimosa. We cut the GO/RGO-3 bilayer film into a flower shape. After that, we attached the GO/RGO-3 bilayer flower to a tube which is used to control the humidity changes around our graphene flower (Figure 4b; Video S1, Supporting

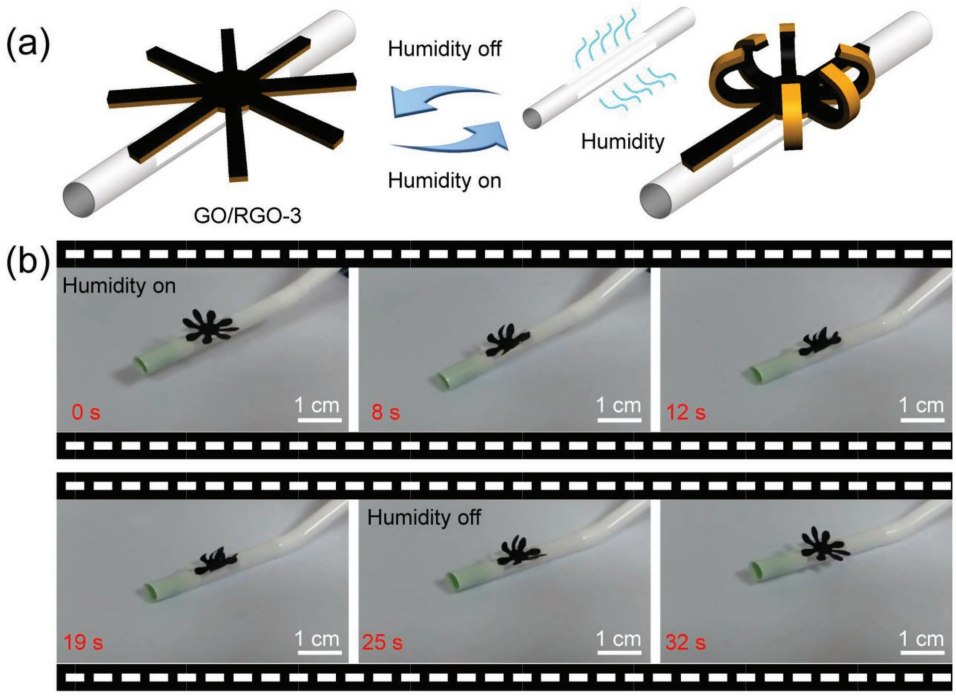

Figure 4. Humidity-responsive performance of our smart mimosa. a) Flower shape was cut and attached on a tube. The tube is used to control surroundings humidity, in which two holes were cut for humidity spreading. b) The flower can be manipulated by changing surroundings humidity.

Information). After 12 s of humidity on, the flower fully closed from the flat state. In addition, the flower opens after the humidity off at 25 s. It took about 7 s to recover to its original state. The second actuator mimics insects. It is well known that arthropods usually have the ability to crawl and carry foods due to the synergy between different curvatures of their legs. Inspired by arthropods (**Figure 5**a), humidity/thermal/light-responsive graphene "insect" was designed and prepared by combining with different responsive property GO/RGO ribbons. As we demonstrated previously, GO/RGO-4 film has the larger curvature than GO/RGO-2 in certain humidity/thermal/light. Therefore, the GO/RGO-2 ribbons can be used as legs to crawl and the GO/RGO-4 ribbons can be used as chela to carry things. These were assembled with a simple paper skeleton to form an integrated humidity/thermal/light-responsive graphene insect. As shown in Figure 5b (Video S2, Supporting Information), in the beginning, we put a green tube below the GO/RGO-4 ribbons. When the light was on and humidity was off, it took about 3.3 s for the GO/RGO-2 and GO/RGO-4 ribbons changing from curled state to straight state, the right GO/RGO-2 legs moved forward, and the position of paper became lower. At that time, when the light was off and humidity was on, GO/RGO-2 and GO/RGO-4 ribbons changed from straight state to curled state, and the left GO/RGO-2 legs moved forward and pushed the green tube forward. Figure 5c shows the horizontal displacement of test point 1 versus time. After five cycles, the whole graphene actuator moved about 2.84 cm in 26 s. Additionally, Figure 5d shows the vertical displacement of test point 1 versus time. Figure 5e shows the horizontal displacement of test point 2 versus time. After five cycles, the whole green tube moved about 3 cm in 24 s.

In conclusion, multiresponsive graphene actuators have been successfully fabricated by sequential vacuum filtration of GO and RGO from aqueous solutions. By controlling the reduction degree of the RGO samples, the reduction gradient of the resultant GO/RGO bilayers could be continuously tuned. Since the presence of OCGs on the GO sheets dominates the interaction with water molecules, the asymmetric GO/RGO bilayers that bear different OCG contents may have distinct water adsorption capacity on each side. Therefore, a mismatch in swelling degree directly leads to the curving of the bilayer toward the RGO side. In this work, we tailor the reduction degree beforehand, so GO/RGO bilayer actuators with tunable deforming variation have been successfully fabricated. The responsive properties have been investigated with care. A maximum curvature of 4.1 cm^{-1} has been achieved, and the response/recover times are only 12 and 6 s, respectively. Since the thermal or photothermal effect can accelerate water desorption, the bilayer actuators are also responsive to heat and light. Using these GO/RGO bilayer actuators as basic components, multiresponsive paper robots that mimic the mimosa and insects have been demonstrated.

Experimental Section

Preparation of GO and RGO Aqueous Solutions: GO was prepared from purified natural graphite (Aldrich, <150 µm) by following the Hummers' method. To remove the residual ions, the GO aqueous solution was washed for several times. The as-synthesized GO solution was collected by centrifugation and then redispersed in distilled water at a concentration of 1 mg mL^{-1} with the aid of ultrasonic treatment. Then, a 500 W medium pressure mercury lamp (characteristic

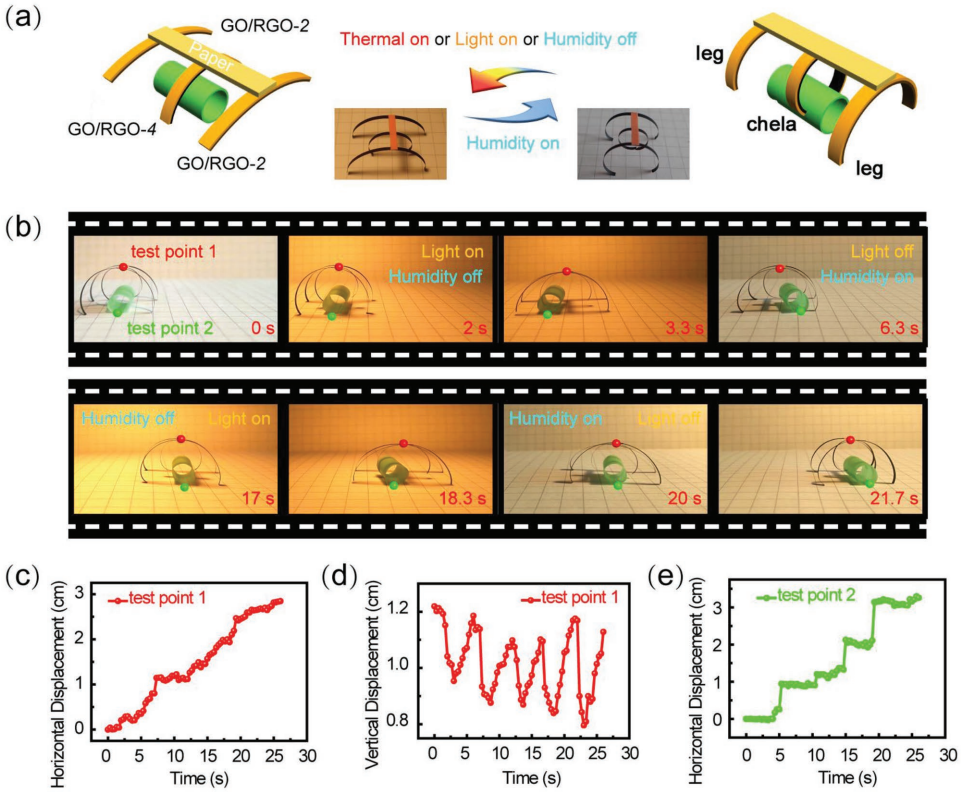

Figure 5. Humidity-, thermal-, and light-responsive performance of our graphene "insect." a) Schemes for the graphene "insect" responding to surroundings humidity, thermal, and light changes. Both ends used GO/RGO-2 ribbons as legs for crawling and the middle was integrated with GO/RGO-4 ribbons as chela for grasping. Three ribbons curl differently under high humidity (97% RH, right images) and become straight under high light power (97% RH, left images). b) The graphene "insect" was manipulated by surroundings humidity and light changes. Each grid is 5 mm. c) The horizontal displacement of the test point 1 versus time in panel (b). d) The vertical displacement of the test point 1 versus time in panel (b). e) The horizontal displacement of the tube (test point 2) versus time in panel (b).

wavelength, 365 nm) was used as a UV light source to reduce GO in aqueous solutions in a photochemical manner. The distance between the light source and the sample was 8 cm. For the RGO samples with different reduction degrees, the GO aqueous solutions were irradiated by UV light for 1–4 h at room temperature, respectively. The resultant RGO samples were designated as RGO-*x*, where *x* is the photoreduction time (hour).

Preparation of GO/RGO Film: First, RGO films were prepared by vacuum filtration of the RGO-*x* aqueous solutions. After that, without drying the RGO film, a GO solution was casted into the funnel for continuous vacuum filtration. In this way, a GO/RGO bilayer film formed after air drying at room temperature. Finally, the GO/RGO-*x* bilayer films were peeled off for further use. For the moisture-responsive tests, the GO/RGO-*x* bilayer films were cut into ribbons with a width of 1.0 mm and a length of 12.0 mm.

Characterization: SEM images were obtained using a JEOL JSM-7500 field-emission scanning electron microscope (FE-SEM). XPS was performed on an ESCALAB 250 spectrometer. The controlled humidity environments were achieved using saturated aqueous solutions of $MgCl_2$, K_2CO_3, NaBr, NaCl, KCl, and K_2SO_4 in a closed glass vessel, which yielded ≈33%, 44%, 57%, 75%, 86%, and 97% RH, respectively.

Supporting Information

Supporting Information is available from the Wiley Online Library or from the author.

Acknowledgements

This work was supported by the National Key Research and Development Program of China and National Natural Science Foundation of China (NSFC) under Grant Nos. #2017YFB1104300, #61522503, #61590930, #61775078, and #61605055. Scientific and Technological Developing Scheme of Jilin Province Nos. #20180101061JC. This article is part of the special series on *Advanced Intelligent Systems* that showcases the outstanding achievements of leading international researchers on intelligent systems.

Conflict of Interest

The authors declare no conflict of interest.

Keywords

actuators, biomimetic, graphene oxide, multiresponse, reduction gradient

Received: July 11, 2018
Revised: August 11, 2018
Published online: September 6, 2018

[1] a) J. You, J. S. Heo, J. Kim, T. Park, B. Kim, H. S. Kim, Y. Choi, H. O. Kim, E. Kim, *ACS Nano* **2013**, *7*, 4119; b) J. H. Son, B. Cho, S. Hong, S. H. Lee, O. Hoxha, A. J. Haack, L. P. Lee, *Light: Sci. Appl.* **2015**, *4*, 280; c) S. Juodkazis, *Nat. Photonics* **2016**, *10*, 499; d) D. D. Han, Y. L. Zhang, J. N. Ma, Y. Liu, J. W. Mao, C. H. Han, K. Jiang, H. R. Zhao, T. Zhang, H. L. Xu, H. B. Sun, *Adv. Mater. Technol.* **2017**, *2*, 9.

[2] a) K. S. Lee, P. N. Prasad, G. Huyet, C. H. Tan, *Opt. Express* **2012**, *20*, 10721; b) K. R. Choudhury, W. J. Kim, Y. Sahoo, K. S. Lee, P. N. Prasad, *Appl. Phys. Lett.* **2006**, *89*, 3; c) B. Kim, H. Shin, T. Park, H. Lim, E. Kim, *Adv. Mater.* **2013**, *25*, 5483; d) S. Hong, M. Y. Lee, A. O. Jackson, L. P. Lee, *Light: Sci. Appl.* **2015**, *4*, 267; e) M. Malinauskas, A. Zukauskas, S. Hasegawa, Y. Hayasaki, V. Mizeikis, R. Buividas, S. Juodkazis, *Light: Sci. Appl.* **2016**, *5*, 14; f) D. Thuau, K. Kallitsis, F. D. Dos Santos, G. Hadziioannou, *J. Mater. Chem. C* **2017**, *5*, 9963.

[3] a) K. Kumar, K. K. C. Lee, J. Z. Li, J. Nogami, N. P. Kherani, P. R. Herman, *Light: Sci. Appl.* **2014**, *3*, 7; b) D. H. Gracias, *Curr. Opin. Chem. Eng.* **2013**, *2*, 112; c) D. D. Han, Y. L. Zhang, J. N. Ma, Y. Q. Liu, B. Han, H. B. Sun, *Adv. Mater.* **2016**, *28*, 8328.

[4] a) M. Jamal, A. M. Zarafshar, D. H. Gracias, *Nat. Commun.* **2011**, *2*, 6; b) J. S. Randhawa, K. E. Laflin, N. Seelam, D. H. Gracias, *Adv. Funct. Mater.* **2011**, *21*, 2395; c) K. Ariga, Q. M. Ji, J. P. Hill, Y. Bando, M. Aono, *NPG Asia Mater.* **2012**, *4*, 11; d) K. Ariga, Q. M. Ji, W. Nakanishi, J. P. Hill, M. Aono, *Mater. Horiz.* **2015**, *2*, 406.

[5] a) E. Gultepe, J. S. Randhawa, S. Kadam, S. Yamanaka, F. M. Selaru, E. J. Shin, A. N. Kalloo, D. H. Gracias, *Adv. Mater.* **2013**, *25*, 514; b) K. Malachowski, J. Breger, H. R. Kwag, M. O. Wang, J. P. Fisher, F. M. Selaru, D. H. Gracias, *Angew. Chem., Int. Ed.* **2014**, *53*, 8045; c) C. L. Randall, E. Gultepe, D. H. Gracias, *Trends Biotechnol.* **2012**, *30*, 138.

[6] a) L. Zhang, E. Ruh, D. Grutzmacher, L. X. Dong, D. J. Bell, B. J. Nelson, C. Schonenberger, *Nano Lett.* **2006**, *6*, 1311; b) L. Dai, L. Zhang, *Nanoscale* **2013**, *5*, 971; c) N. Hu, X. Han, S. Huang, H. M. Grover, X. Yu, L. N. Zhang, I. Trase, J. X. J. Zhang, L. Zhang, L. X. Dong, Z. Chen, *Nanoscale* **2017**, *9*, 2958.

[7] J. H. Na, A. A. Evans, J. Bae, M. C. Chiappelli, C. D. Santangelo, R. J. Lang, T. C. Hull, R. C. Hayward, *Adv. Mater.* **2015**, *27*, 79.

[8] a) W. Xiong, Y. Liu, L. J. Jiang, Y. S. Zhou, D. W. Li, L. Jiang, J. F. Silvain, Y. F. Lu, *Adv. Mater.* **2016**, *28*, 2002; b) W. Xiong, Y. S. Zhou, W. J. Hou, L. J. Jiang, Y. Gao, L. S. Fan, L. Jiang, J. F. Silvain, Y. F. Lu, *Sci. Rep.* **2014**, *4*, 6; c) H. B. Jiang, Y. L. Zhang, D. D. Han, H. Xia, J. Feng, Q. D. Chen, Z. R. Hong, H. B. Sun, *Adv. Funct. Mater.* **2014**, *24*, 4595; d) C. D. Wang, J. L. Xu, M. F. Yuen, J. Zhang, Y. Y. Li, X. F. Chen, W. J. Zhang, *Adv. Funct. Mater.* **2014**, *24*, 6372; e) X. L. Lu, W. M. Munief, F. Heib, M. Schmitt, A. Britz, S. Grandthyl, F. Muller, J. U. Neurohr, K. Jacobs, H. M. Benia, R. Lanche, V. Pachauri, R. Hempelmann, S. Ingebrandt, *Adv. Mater. Technol.* **2018**, *3*, 14.

[9] a) N. V. Medhekar, A. Ramasubramaniam, R. S. Ruoff, V. B. Shenoy, *ACS Nano* **2010**, *4*, 2300; b) A. M. Dimiev, L. B. Alemany, J. M. Tour, *ACS Nano* **2013**, *7*, 576; c) Z. F. Wan, E. W. Streed, M. Lobino, S. J. Wang, R. T. Sang, I. S. Cole, D. V. Thiel, Q. Li, *Adv. Mater. Technol.* **2018**, *3*, 19.

[10] H. Okuzaki, H. Suzuki, T. Ito, *J. Phys. Chem. B* **2009**, *113*, 11378.

[11] H. Okuzaki, T. Kuwabara, K. Funasaka, T. Saido, *Adv. Funct. Mater.* **2013**, *23*, 4400.

[12] H. Okuzaki, K. Hosaka, H. Suzuki, T. Ito, *React. Funct. Polym.* **2013**, *73*, 986.

[13] H. C. Bi, K. B. Yin, X. Xie, J. Ji, S. Wan, L. T. Sun, M. Terrones, M. S. Dresselhaus, *Sci. Rep.* **2013**, *3*, 7.

[14] F. Zhao, Y. Liang, H. H. Cheng, L. Jiang, L. T. Qu, *Energy Environ. Sci.* **2016**, *9*, 912.

[15] H. H. Cheng, Y. Hu, F. Zhao, Z. L. Dong, Y. H. Wang, N. Chen, Z. P. Zhang, L. T. Qu, *Adv. Mater.* **2014**, *26*, 2909.

[16] R. K. Joshi, P. Carbone, F. C. Wang, V. G. Kravets, Y. Su, I. V. Grigorieva, H. A. Wu, A. K. Geim, R. R. Nair, *Science* **2014**, *343*, 752.

[17] H. H. Cheng, J. Liu, Y. Zhao, C. G. Hu, Z. P. Zhang, N. Chen, L. Jiang, L. T. Qu, *Angew. Chem., Int. Ed.* **2013**, *52*, 10482.

[18] a) D. D. Han, Y. L. Zhang, H. B. Jiang, H. Xia, J. Feng, Q. D. Chen, H. L. Xu, H. B. Sun, *Adv. Mater.* **2015**, *27*, 332; b) D. D. Han, Y. L. Zhang, Y. Liu, Y. Q. Liu, H. B. Jiang, B. Han, X. Y. Fu, H. Ding, H. L. Xu, H. B. Sun, *Adv. Funct. Mater.* **2015**, *25*, 4548.

